

Rheological studies on concentrated solutions of heterocyclic polymers

C. -P. Wong and G. C. Berry

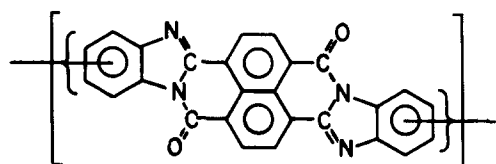
Department of Chemistry, Carnegie-Mellon University, Pittsburgh, PA 15213, USA

(Received 31 July 1978)

The rheological properties of two related heterocyclic polymers are studied in concentrated solutions. One of these (BBB) is a flexible chain polymer, whereas the other (BBL) is a rigid ladder polymer. Data are presented both on solutions in anhydrous acids and in slightly wet acids. In the latter case the effects of reversible intermolecular association are analyzed and compared for BBB and BBL. It is found that low degrees of association have a profound difference on the rheological properties of solutions of the two polymers. For example, a yield behaviour is observed with solutions of BBL, whereas comparable association with BBB appears to result in random (reversible) crosslinking, forming a branched polymer. The creep and recovery behaviour of BBB in anhydrous solutions is found to have much in common with the behaviour of more familiar flexible chain polymers, including a total strain criterion for the onset of non-linear creep.

INTRODUCTION

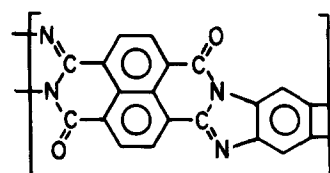
Intermolecular association is sometimes suspected when anomalous behaviour is found in the rheological properties of polar polymers or their concentrated solutions. It is often difficult to assess this suspicion since the association may either be difficult to disrupt or be reduced only by increasing the temperature, which will usually have a pronounced effect on the rheological properties even if intermolecular association is not an important factor. In our studies on the rheological properties of concentrated solutions of the heterocyclic polymer polybisbenzimidazobenzophenanthroline-dione (BBB)¹ in strong protic acids it was found that reversible association could be induced by the action of very small amount of water².



BBB

Here, we will describe some rheological properties of the dry solutions and the reversible effects on these produced by a small amount of water. The action of water is interpreted in terms of an aggregate structure created when the polymer, which is highly protonated in the strong acids, undergoes association as it deprotonates slightly by virtue of the higher basicity of water.

The effect of a small amount of water on the rheological properties of a ladder polymer with a chemical structure similar to BBB serves as a counterpoint to the studies on BBB, illustrating effects due to intramolecular rigidity that are absent in the behaviour of the flexible BBB polymer. The ladder polymer poly[7-oxo-7,10 *H*-benz-de]imidazo[4',5':5,6]-benzimidazo(2,1-*a*)isoquinoline-3,4:10,11-tetrayl]-10-carbonyl 1], BBL³, is used in these studies.



BBL

EXPERIMENTAL

Materials

The BBB polymer used here has been described previously^{1,2,4-6}. An unfractionated sample of polymer 51165 with weight-average molecular weight M_w equal to 6.5×10^4 (see ref. 2) was used. The polymer was dried under vacuum at 200°C for several days before use. Previous work has shown that the polymer can be recovered without chemical change from solutions in methane sulphonic acid or in sulphuric acids up to 100% sulphuric acid (chemical modification is effected in fuming sulphuric acid, which was not used for these studies).

The BBL polymer was obtained from F. E. Arnold, (Polymer Branch, Wright-Patterson Air Base, Ohio). An unfractionated sample of the polymer with a weight-average molecular weight of 5.2×10^4 (unpublished light scattering data) was used here. The polymer was dried under vacuum at 200°C for several days prior to use.

Methane sulphonic acid was distilled under vacuum (0.05 mmHg) at 105°C and stored under a nitrogen blanket. Analytical grade sulphuric acid (97%) was used as received.

Solutions were prepared by mixing dry polymer and acid in a sealed container at 60°C. A teflon coated magnetic bar was used to slowly stir the solution.

Apparatus

The cone-and-plate rheometer used in these studies has been described in detail elsewhere⁷. Its main features for

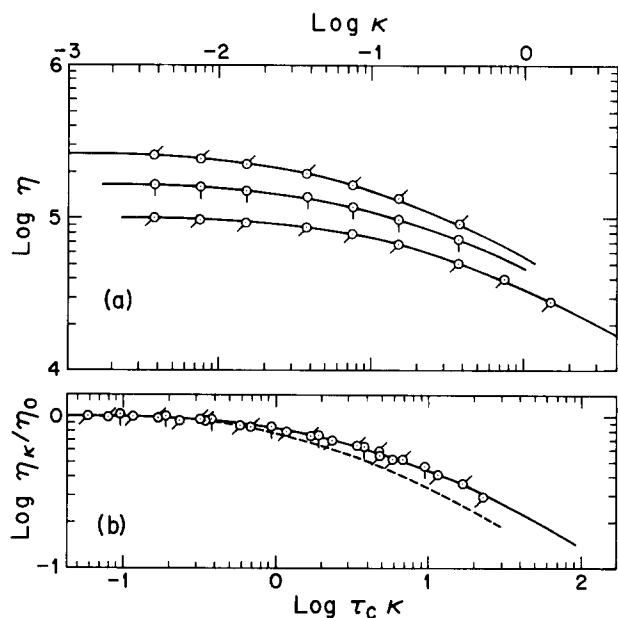


Figure 1 (a) Steady state viscosity η plotted logarithmically against rate of shear κ for a solution of BBB in MSA ($M_w = 6.5 \times 10^4$, $c = 0.175$ g/ml) at three temperatures. Key: Pip clockwise from two o'clock: 24.0°, 32.8°, and 41.2°C. (b) Reduced plot η_κ/η_0 versus $\tau_c \kappa$; broken curve, PIB/cetane

this work include (1) a gold cone-and-plate to provide an inert surface; (2) a sample chamber designed to permit close control of the sample environment; (3) the ability to perform creep, recovery and steady state flow measurements over a wide range of shear stresses.

The sample chamber and an attached glove bag were purged with dry argon before the sample was transferred from its sealed container to the sample chamber via the glove bag.

The sample chamber was continuously purged with a slow flow of argon (500 to 1500 ml/min, see below). In some experiments the argon was passed through a cryostat (1 l in volume) in which a layer of ice deposited on the vessel wall was held at temperature T_{CRY} . The argon was then passed through a chamber containing a vial with a pre-weighed aliquot of the sample before being fed to the rheometer chamber and out to a second chamber containing another vial with a pre-weighed aliquot of the sample. Typically, T_{CRY} was in the range -50 to -5°C . This arrangement permitted reasonable control of the partial pressure of water in the slightly wet argon stream, and a check on the partial pressure in the inlet and outlet streams of the sample environment chamber.

An attenuated total reflectance (ATR) apparatus was constructed to permit observation of the visible spectrum of a concentrated solution of BBB in a strong acid as the solution slowly absorbed water. The apparatus is equipped with a right-angle sapphire prism for single pass reflectance, and is designed to fit into a Cary Spectrophotometer (Model 14). The apparatus is fitted with quartz windows and can be sealed to provide a well controlled sample environment. The specimen, coated (or pressed if a solid) on the 1.0×1.1 cm face of the prism, is usually about 0.5 mm thick and is held in place by a glass slide placed parallel to the prism face.

RESULTS

Rheological behaviour of a dry solution of BBB

A solution with 0.121 weight fraction polymer in methane sulphonic acid was examined over the temperature range

24.0° to 41.2°C under constant dry argon flow. In addition, vials of anhydrous methane sulphonic acid placed close to the sample helped to maintain the solution in a (nearly) water free state. Measurements included the strain $\gamma(t)$ as a function of time with a constant shear stress σ impressed on the sample, and the recovered strain or recoil $\gamma_R(S, \theta)$ as a function of the time θ of recovery after the stress was removed following creep for a time S under a constant stress σ . The latter data are conveniently expressed as a recovery function $R_\sigma(S, \theta)$ defined as

$$R_\sigma(S, \theta) = \frac{\gamma_R(S, \theta)}{\sigma} \quad (1)$$

In the limit as S becomes large and the creep approaches a steady-state flow, the creep data give the viscosity $\eta_\kappa = \sigma/\kappa$ at a rate of strain κ , where κ is the limiting value of $d\gamma(t)/dt$ at long time. The total recovery function $R_\sigma(\infty, \infty)$ measured after steady-state flow is denoted simply by R_κ . The data on η_κ as functions of κ at three temperatures are shown in Figure 1a. As shown in Figure 1b, the data on η_κ can all be reduced to a single function by a relation of the form

$$\eta_\kappa/\eta_0 = Q(\tau_c \kappa) \quad (2)$$

where τ_c is a characteristic time defined by the relation

$$\tau_c = \eta_0 R_0 \quad (3)$$

Here, R_0 is the limiting value of R_κ for small κ , or the linear steady-state compliance often denoted J_e^0 , equal to 1.84×10^{-4} cm²/dyn at 48.9°C for the data shown. Although use of a reduction parameter like τ_c has precedence both experimentally^{4,8-10} and theoretically¹¹, such a correlation has not been used very often owing to a paucity of data on R_0 . Data for a solution of polyisobutylene (PIB) in cetane are shown as a dashed curve in Figure 1b to illustrate our observation¹² that plots of η_κ/η_0 versus $\tau_c \kappa$ are usually similar at small $\tau_c \kappa$ for materials that may differ in polymer structure, concentration or molecular weight polydispersity — this correspondence is not obtained, for example, if η_κ is correlated with κ , $\eta_0 \kappa$ or $\eta_\kappa \kappa$. Moreover, plots of η_κ/η_0 versus $\tau_c \kappa$ are similar over a wide range in $\tau_c \kappa$ for diverse materials if their molecular weight distribution is similar.

The empirical form found for the function $Q(\tau_c \kappa)$ with the data on BBB happens to correspond within experimental error to the function $Q(\tau_0 \kappa)$ calculated by Graessley¹³ for a linear polymer with a logarithmic-normal molecular weight distribution if we put the relaxation time τ_0 of Graessley equal to $0.138 \tau_c$.

It will sometimes be convenient to introduce a shift factor a_T defined by

$$a_T = (\tau_c)_T / (\tau_c)_{T^*} \quad (4)$$

where T^* is some convenient arbitrary temperature.

Since $\eta_0(T)$ is accurately given by the Vogel relation

$$\eta_0 \propto \exp \left[\frac{C}{(T - T_0)} \right] \quad (5)$$

for solutions of BBB in MSA, a_T can be calculated given C and T_0 for the concentration of interest if it is assumed that

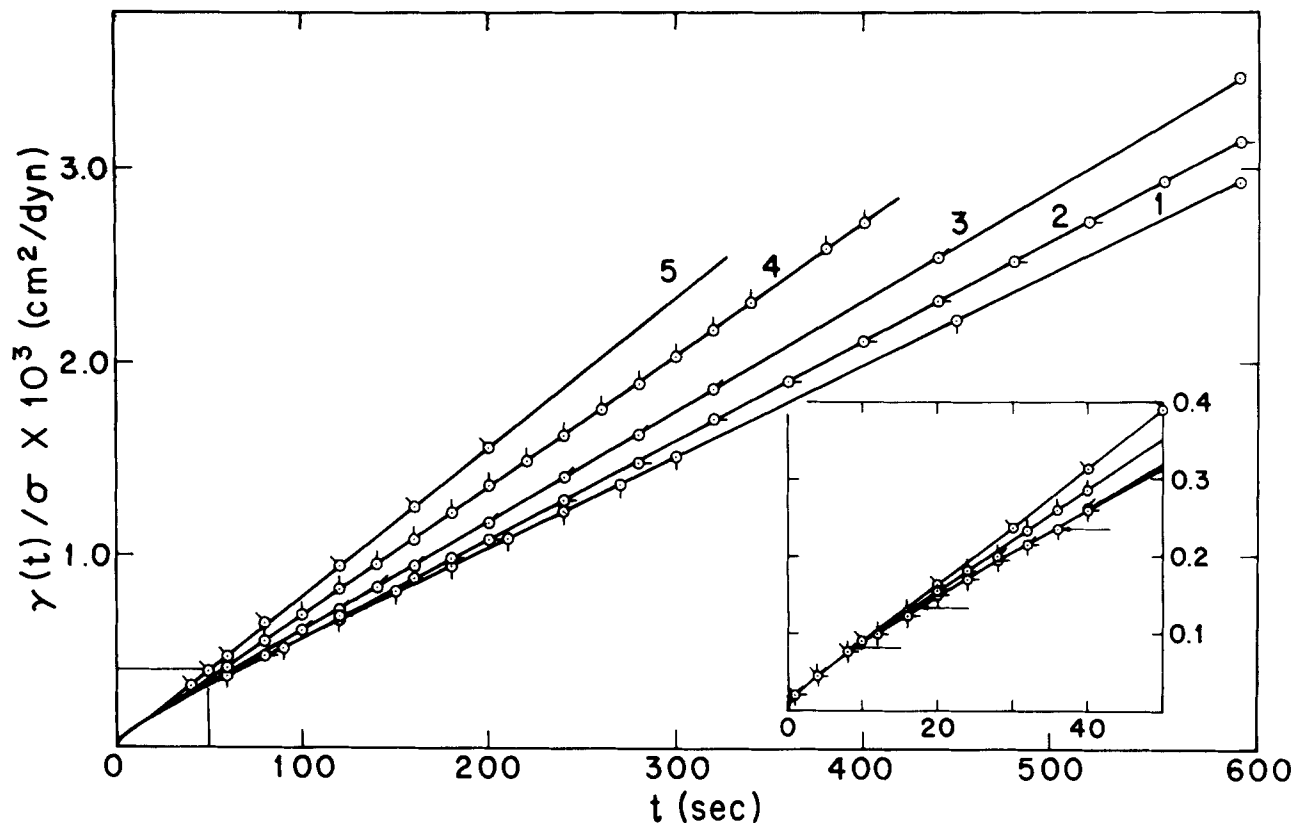


Figure 2 The reduced strain $\gamma(t)/\sigma$ plotted logarithmically against time t for the BBB/MSA solution at 24.4°C under five constant imposed shear stress σ , Pip counter-clockwise from six o'clock: 8.0×10^2 , 2.90×10^3 , 6.41×10^3 , 1.12×10^4 and 1.83×10^4 dyne cm^{-2} . Small rectangle at the lower left corner is magnified at the right hand side. The arrows indicate the time when the strain reached γ^* for each σ

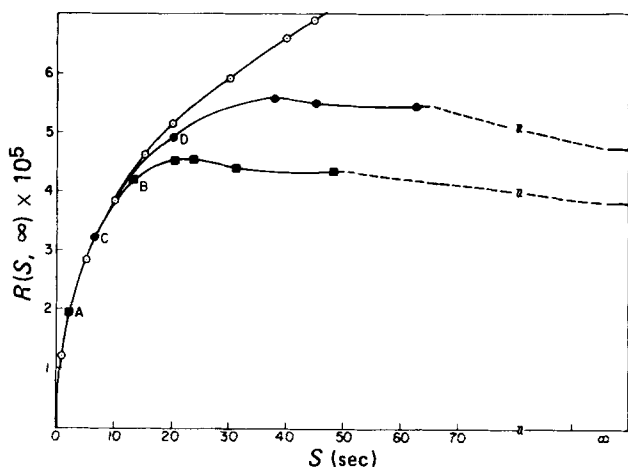


Figure 3 Total recoverable compliance $R(S, \infty)$ plotted against the time of creep S for the BBB/MSA solution at 23.6°C at three stress levels: \circ , 880; \bullet , 1.12×10^4 and \blacksquare , 1.83×10^4 dyne cm^{-2}

R_0^{-1} is proportional to $T\rho$. For the concentration used here, $C^{-1} = 3.53 \times 10^{-4}$ and $T_0 = 81\text{K}$.

The data on dry solutions of BBB also exhibit another feature we have found with solutions of vinyl polymers. We have reported elsewhere^{7,12} that the creep properties of concentrated solutions of several polymers appear to be linear for any applied stress σ so long as the total strain on the sample does not exceed a critical value γ^* characteristic of the specimen. Thus, the function $\gamma(t) - \sigma(R_\sigma(t, \infty) + t/\eta_0)$, which is zero if a material obeys the laws of linear viscoelasticity, is found to be zero if $\gamma(t) < \gamma^*$, but to be non-zero if $\gamma(t) > \gamma^*$ provided the stress exceeds a certain value.

The linear and non-linear creep behaviour of a solution of BBB in methane sulphonic acid (0.175 g/ml) is shown in Figure 2. It is seen that the reduced strain $\gamma(t)/\sigma$ appears to be independent of σ at short time, but that an acceleration of creep is observed with the higher stresses at longer time, causing a deviation of $\gamma(t)/\sigma$ from the stress independent function observed for small stresses.

The total recoil measured after a long recovery time following creep of duration S expressed as the compliance $R_\sigma(S, \infty)$ is shown in Figure 3. Data were obtained at two stresses (11 200 and 18 300 dyn/ cm^2) large enough to lead to non-linear behaviour, and at a stress low enough (800 dyn/ cm^2) so that the linear viscoelastic response was obtained. It may be seen that $R_\sigma(S, \infty)$ is independent of σ at small S , but that it passes through a maximum for the experiments at the larger values of σ before reaching the value R_κ observed after steady-state flow.

In addition to $R_\sigma(S, \infty)$, the transient response $R_\sigma(S, \theta)$ was determined as a function of the recovery time θ following creep of duration S corresponding to the points labelled A, B, C and D in Figure 3. The data, shown in Figure 4, are compared with the curve calculated with the Boltzmann superposition principle of linear viscoelasticity in the form

$$R_\sigma(S, \theta) = J(S) - [J(S + \theta) - J(\theta)] \quad (6)$$

It can be seen that the transient data corresponding to points A and C are well fitted by equation (6), whereas equation (6) overestimates the recoil corresponding to points B and D.

The effects of water on solutions of BBB

Small amounts of water have a profound effect on the

properties of solutions of BBB. Indeed, a solution allowed to stand in moist air will absorb water and form a hard gel in a few hours, after which syneresis will develop, with acid being exuded from the gel. Films prepared in this way have been subjected to X-ray diffraction and tensile creep measurement⁶. At the much lower levels of absorbed water of interest in these studies, the absorbed water manifests itself in changes in η_0 , τ_c and the electronic absorption spectrum. The latter was monitored as water slowly diffused into a solution of BBB in methane sulphonic acid (0.176 g/ml) mounted in an enclosed ATR apparatus. The diffusion of water into the ATR apparatus and then into the sample over a period of 24 h produced a visible change in the colour of the sample. The change was slow, and appeared to occur uniformly across the 1.0 cm width of the sample. The ATR spectra given in Figure 5 measured over a 24 h

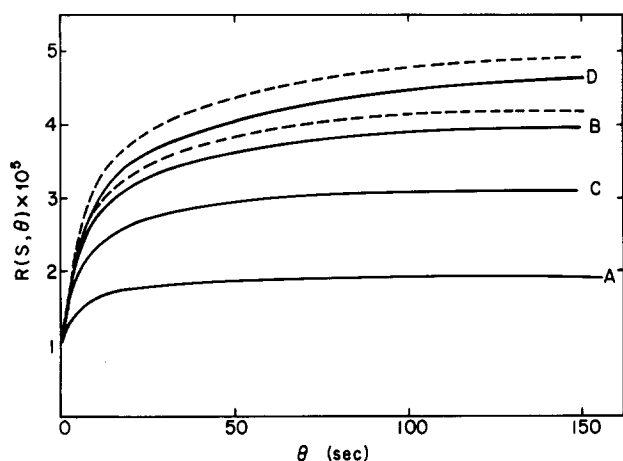


Figure 4 Transient recovery $R(S, \theta)$ plotted against the recovery time θ following creep of duration S , solid line, experimental; broken line, constructed according to equation (6). Lines coincide for curves A and C

period show the gradual shift of the spectrum to longer wavelengths. This shift is in accord with behaviour reported previously for dilute solutions of Vat Red 15 (Colour Index 71100), a model compound for the BBB repeating unit, which was studied to obtain a pK_B value of -7 in sulphuric acid containing up to ten percent water. Measurements of the freezing point depression of solutions of Vat Red 15 and BBB in sulphuric acid show that both are multiply protonated⁵. Thus, the spectral shift observed when a solution of BBB or Vat Red 15 in sulphuric and/or methane sulphonic acid absorbs water can be ascribed to the effects of partial deprotonation of the solute and, perhaps, association of the deprotonated solute.

Since we will ultimately be interested in solutions of BBB in strong acids in equilibrium with a vapour containing a small amount of water, it is pertinent to consider the uptake of water by an acid in some detail. At the low levels of moisture uptake of interest here, the sorption by the acid of water from a wet gas can be considered to involve simultaneous condensation (or evaporation) of water at the gas-liquid interface and diffusion of the water in the liquid away from the interface. Under these conditions the total amount M_t of liquid absorbed by a semi-infinite plane slab of thickness l after time t of exposure is given by¹⁵

$$M_t = M_\infty \left(1 - \sum_{n=1}^{\infty} \frac{2L^2 \exp(-\beta_n^2 Dt/l^2)}{\beta_n^2 (\beta_n^2 + L^2 + L)} \right) \quad (7)$$

Here M_∞ is the limiting value of M_t at infinite time, L is equal to $l\alpha/D$ where α and D are the condensation coefficient of water and the diffusion constant of water in the liquid, respectively, both assumed to be independent of the water content of the acid at the water concentrations of interest here, and the β_n are the positive roots of the equation

$$\beta_n \tan \beta_n = L$$

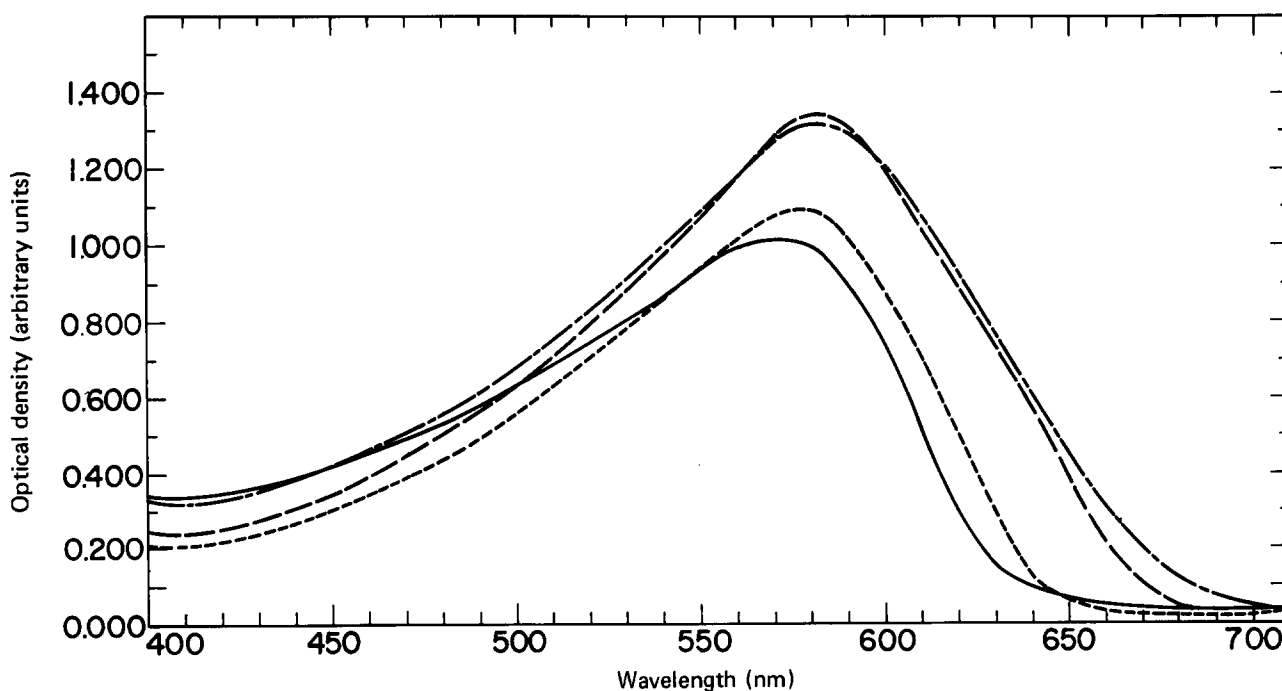


Figure 5 ATR spectra of the BBB/MSA solution at room temperature at various aging times: — zero, --- 10 h, - - - 17.5 h and - · - 24.0 h

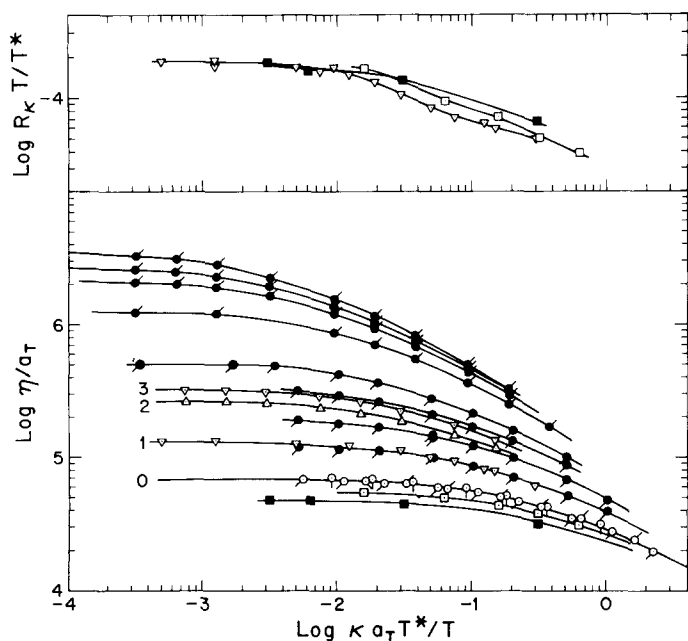


Figure 6 Total recoverable compliance R_k and steady state viscosity η plotted logarithmically against rate of shear κ for the BBB/MSA solution with increasing amount of moisture content. All curves reduced to $T^* = 48.9^\circ\text{C}$ as shown on the ordinate and abscissa in labels. Curve 0, reduced from Figure 1a; curves 1, 2, and 3, moist argon passed over ice at -34°C , -13.6°C and -7.6°C respectively; filled square, dry sample; the rest, various moisture contents. Original temperature key: filled square 32.2° , opened square 23.8° , filled circle pip 8 o'clock, 42.9° and pip 2 o'clock 32.1° ; and triangle 48.9°C

Inspection of plots of $\log(M_t/M_\infty)$ versus $\log(Dt/l^2)$ calculated at constant L with equation (7) show that these become parallel to each other for $L < 0.1$.

Data obtained for the sorption of water by a BBB solution (0.121 wt. fraction polymer in 97 percent sulphuric acid) at 25.5°C were in good agreement with curves for $\log(M_t/M_\infty)$ versus $\log Dt/l^2$ calculated with equation (7) for the limiting case $L < 0.1$. With the estimate $4.4 \times 10^{-7} \text{ cm}^2/\text{sec}$ for the diffusion constant of water in the sulphuric acid at 25°C (based on the conductances $\lambda_{\text{H}_3\text{O}^+}^0 = 1.08$ and $\lambda_{\text{HSO}_4}^0 = 170 \text{ cm}^2\Omega^{-1}\text{mol}^{-1}$ for hydronium ion and bisulphate ion, respectively, given by Sidebottom and Spiro¹⁶) a direct comparison of the experimental data with equation (7) yields $\alpha/D = 0.0031$, or $\alpha = 2.8 \times 10^{-8} \text{ cm/sec}$. The very small value of α/D shows that the condensation of the water at the gas-liquid interface is the limiting step in the water sorption at the experimental conditions studied. Under these conditions, to a good approximation, equation (7) reduces to

$$\frac{C(t) - C_0}{C_\infty - C_0} = \frac{M_t}{M_\infty} = 1 - \exp(-\alpha t/l) \quad (8)$$

in which the concentration of water within the slab is uniform. A similar relation for diffusion into a sphere of radius a in the limit when $\alpha a/D$ is small given by equation (8) with l replaced by $a/3$ will find use below.

Water has a far more pronounced effect on the viscosity and the flow curve than on the ATR spectrum, with η_0 increasing one hundred-fold in some cases over a period of weeks as the solution slowly absorbed water. Data for η_k and R_k determined at 48.9°C with a solution of BBB in methane sulphonic acid after exposure for several days to dry argon passed over ice at -34.4° , -13.6° and -7.6°C (vapour

pressure of water 0.180, 1.411 and 2.408 mmHg, respectively) are displayed in Figure 6 (curves 1, 2 and 3). The water uptake in the aliquots in the argon stream was found to be 1.2 wt % – this is much less water than would be absorbed by sulphuric acid under similar conditions. Inspection of Figure 7 shows that moist argon has a marked effect on η_k , but only slightly affects R_k . The absorption is slow enough that the water concentration within the cone and plate gap is probably nearly uniform and given approximately by the modified version of equation (8) for spheres, with a equal to the cone-and-plate radius. Otherwise, an average viscosity $\bar{\eta}$ given by

$$\bar{\eta} = \frac{3}{a^3} \int_0^a \eta(r) r^2 dr \quad (9)$$

is measured. The weighting of the radial dimension in this average tends to make $\bar{\eta}$ most sensitive to the water content near the perimeter of the solution in the cone and plate gap.

Some data were collected for η_k as a function of the time exposed to moist argon without systematic determination of R_k or the uptake of water in the aliquots. These data are also included in Figure 6, all data having been reduced to 48.9°C with a_T as indicated. (Some experimental points of R_k are omitted for clarity, but these are included below.) The data discussed in the previous section (curve 0) are seen to lie above the lowest curve by about 45% indicating the presence of a small amount of water. Overall, the maximum increase in η_k observed is seen to be nearly one hundred-fold, whereas only a small change in R_k is observed.

All of the data in Figure 6 are replotted in Figure 7 as reduced curves of η_k/η_0 and R_k/R_0 versus $\tau_c \kappa$. In constructing Figure 7, τ_c was calculated with experimental R_0 where the latter were available. Otherwise, R_0 was estimated for future use from the necessary shift factor τ_c and η_0 . The behaviour of the PIB solution in cetane mentioned above is also included as the broken line for comparison. All of the data on BBB reduce to a single curve. As mentioned above, the reduced flow curve $Q(\tau_c \kappa)$ matches that calculated by Graessley¹³ for a polydisperse linear polymer with a logarithmic-normal molecular weight distribution if we put Graessley's τ_0 equal to $0.138 \tau_c$.

In one set of experiments included in Figure 7 the dry argon flow rate was stopped for a period and then restarted at a higher than normal rate. As shown in Figure 8, η_0 and $R_0 = \tau_c \eta_0^{-1}$, were both found to increase when the argon flow was stopped, reflecting the increased diffusion of atmospheric moisture into the apparatus, whereas both quantities decreased when the dry argon flow was restarted, showing that the effects observed are reversible.

The effects of water on solutions of BBL

The rheological behaviour described above for solutions of BBB, may be contrasted with that observed with a moderately concentrated solution of the related ladder polymer BBL. The flow curve for a dry solution of BBL (conc = 3.09 g/dl, temp = 14°C) is compared with the flow curve for the same solution containing 0.5 wt % water in Figure 9. It can be seen that the presence of the water has a marked effect at low rates of strain, whereas the flow curves nearly merge at higher strain rates. This behaviour is enhanced with a solution containing 1.8% water, as may be seen in

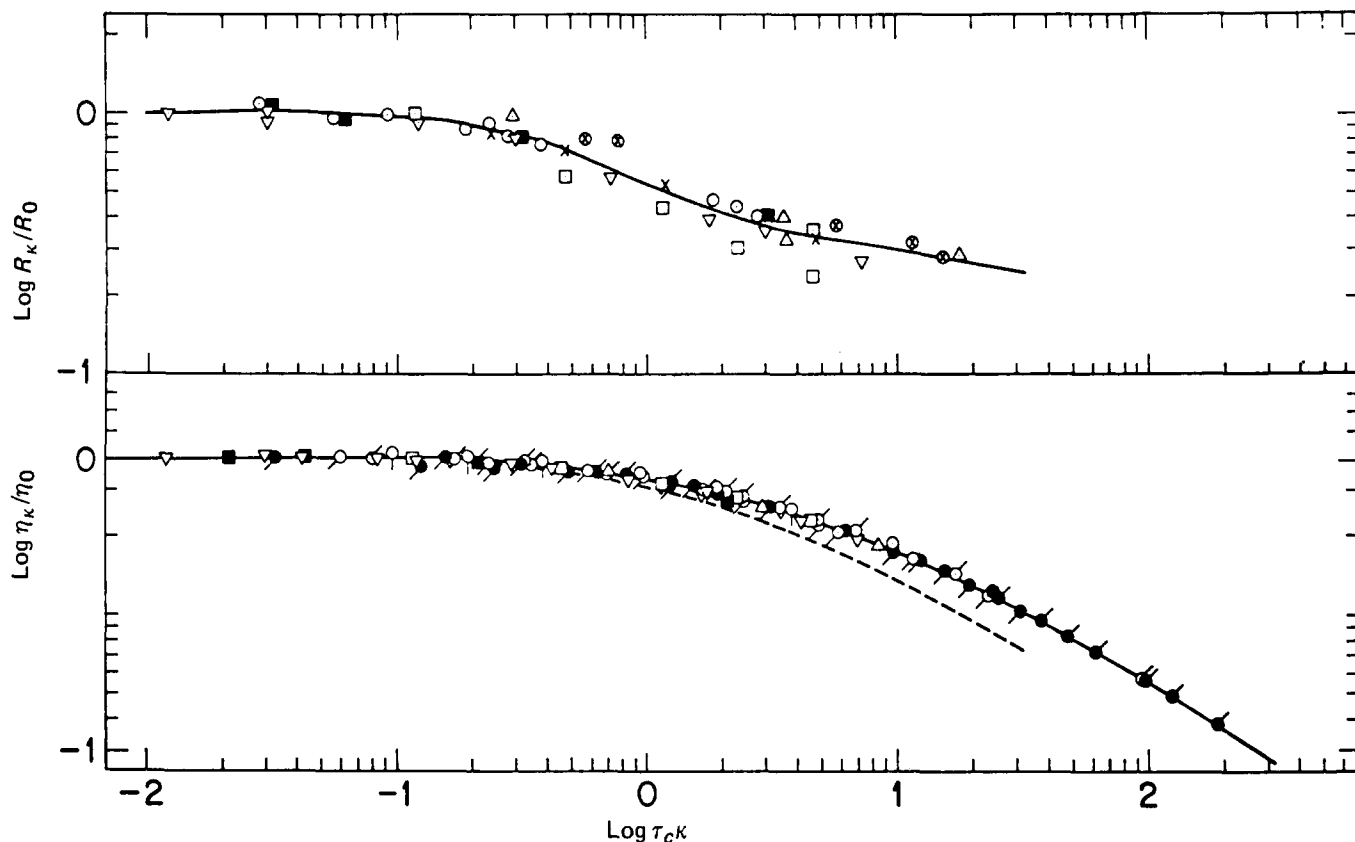


Figure 7 Reduced logarithmic plot of $R_{\kappa}(\infty, \infty)/R_0$ and η_{κ}/η_0 versus $\tau_c \kappa$. Solid line (in viscosity only), Graessley's theoretical curve for a logarithmic-normal molecular weight distribution polymer; broken line, polyisobutylene in cetane with normal molecular weight distribution

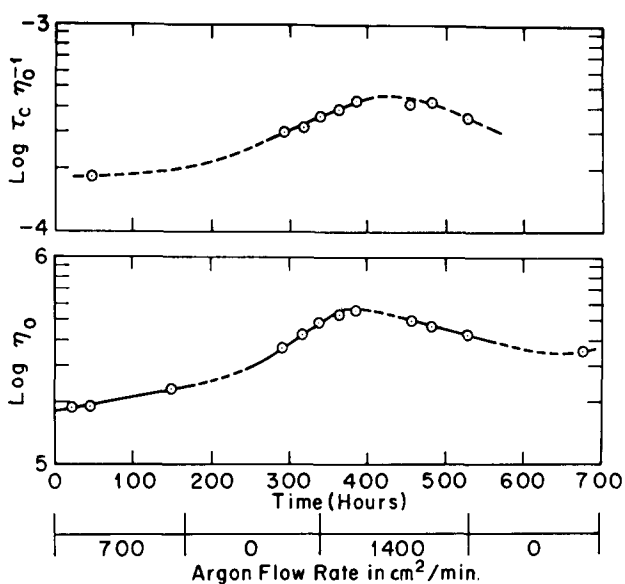


Figure 8 Change of zero shear viscosity η_0 and $\tau_c \eta_0^{-1}$ for the BBB/MSA solution at room temperature as a function of the aging time t . The argon flow rate was varied as indicated on the Figure

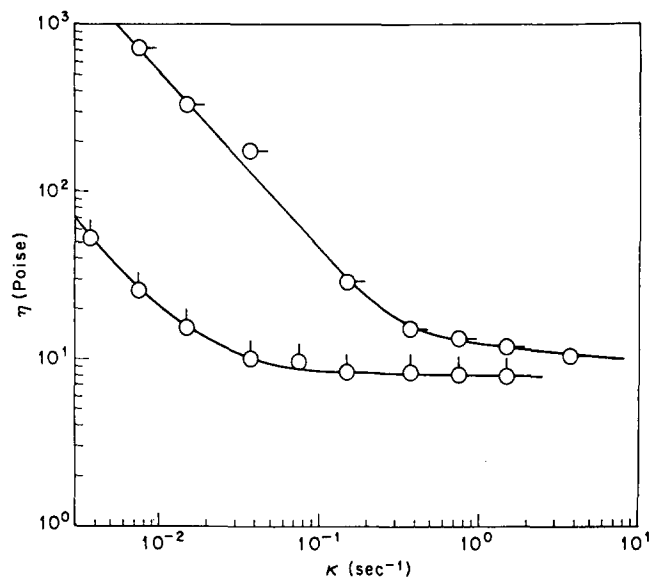


Figure 9 Logarithmic plot of steady state viscosity η against shear rate κ for a 'dry' BBL solution in MSA, \circ , and the same solution with 0.5% water $\circ-$

Figure 10 where η_{κ} is given as a function of κ for data at several temperatures. In this case, the 'plateau' region at high κ was not observed, probably only because high enough rates of strain were not reached.

In addition to the pronounced effect on η_{κ} , the presence of water also produced yield phenomena not observed with BBB solutions with comparable water concentration or with dry BBL solution. The BBL solution with 0.5% water ex-

hibited a yield stress that was detectable, but too small to be measured accurately ($\sim 1-5$ dyn/cm²). On the other hand, the solution with 1.8% water displayed a marked yield behaviour, permitting determination of the elastic shear modulus G_e , at low stress levels, and the stress and strain at the yield point. The elastic modulus is given as a function of temperature in Figure 11. A rheological melting temperature in the range 35°–40°C is observed, with G_e decreasing rapidly with increasing temperature at lower

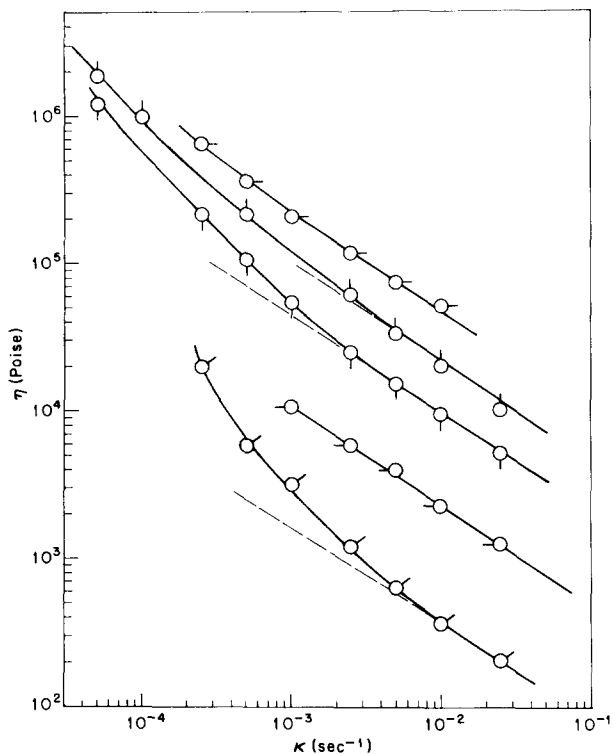


Figure 10 Logarithmic plot of steady state viscosity η versus shear rate κ for a BBL solution in MSA containing 1.8% water at several temperatures, key: Pipclockwise from three o'clock 0.5° , 12.3° , 19.8° , 29.6° and 39.1° C

temperatures (with an apparent activation energy of 35 kcal/mol). The yield stress σ_Y is similarly strongly temperature dependent but the strain γ_Y at yield depends only weakly on temperature, as may be seen in Figure 12. It appears that the yield criterion is nearly one of a limiting total strain.

Although the data are presented above as an elastic modulus, in fact the initial deformation is followed by very slow creep not included in the calculation of G_e . In order to investigate this creep behaviour more thoroughly at strains less than γ_Y , a more concentrated solution of BBL in MSA (3.66 g/dl) was prepared and allowed to slowly absorb water until the water level reached 1.2%. The modulus increased linearly with the water concentration, reaching a level of about 1.4×10^4 dyn/cm² at 20°C. Provided the strain was less than γ_Y in the creep experiment, it was found that the strain was completely recoverable and could be fitted to a cube-root, or Andrade, creep equation^{6,17}:

$$\gamma(t) = \sigma J_A [1 + (t/\tau_A)^{1/3}] \quad (10)$$

where σ is the stress, J_A is the 'instantaneous' compliance obtained by extrapolating $\gamma(t)$ versus $t^{1/3}$ to zero time, and τ_A is the Andrade creep time constant. According to the Boltzmann superposition principle of linear viscoelasticity^{18,19}, the strain in a recovery experiment for material obeying equation (10) is given as a function of the time $\theta = t - S$ following creep of duration S by the equation

$$\gamma(\theta) = \sigma J_A N(S, \theta) \quad (11a)$$

$$N(S, \theta) = (\theta + S)^{1/3} - \theta^{1/3} \quad (11b)$$

The range of strains over which equations (10) and (11) could be tested was small owing to the low value of γ_Y . If

the strain in creep does not exceed γ_Y , then a plot of $\gamma(\theta)/\sigma$ versus $N(S, \theta)$ should pass through the origin and have a slope $J_A/\tau_A^{1/3}$ equal to that of a plot of $\gamma(t)/\sigma$ versus $t^{1/3}$ for the creep data. This behaviour is seen in Figure 13 for one set of data. Experience of other systems⁶ suggests that if the strain in creep exceeds γ_Y so that non-recoverable deformation is obtained, a plot of $\gamma(\theta)/\sigma$ versus $N(S, \theta)$ will intercept the ordinate at a point corresponding to the total non-recoverable strain $\gamma(S) - \sigma J_A [1 + (S/\tau_A)^{1/3}]$ incurred in creep, and may still have a slope nearly equal to the slope

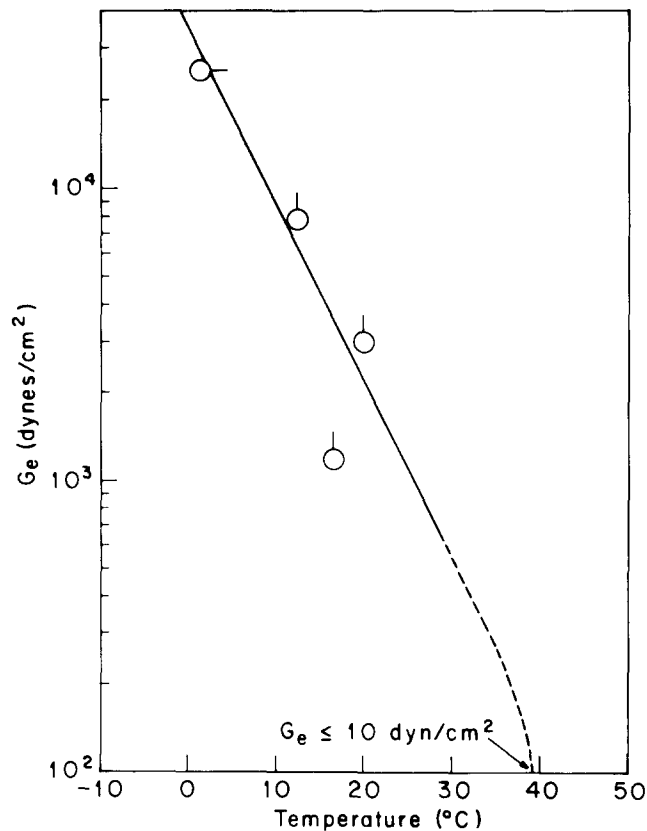


Figure 11 The elastic modulus G_e plotted semilogarithmically against temperature for gels of BBL in MSA containing 1.8% water.

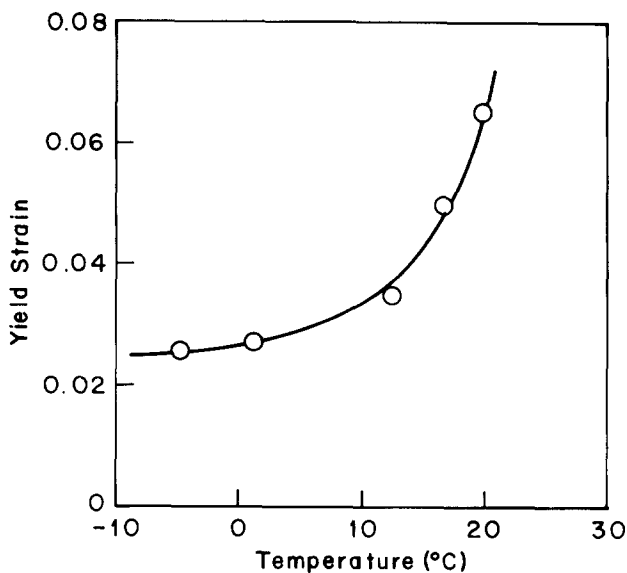


Figure 12 The strain at yield versus temperature for BBL gels in MSA containing 1.8% water

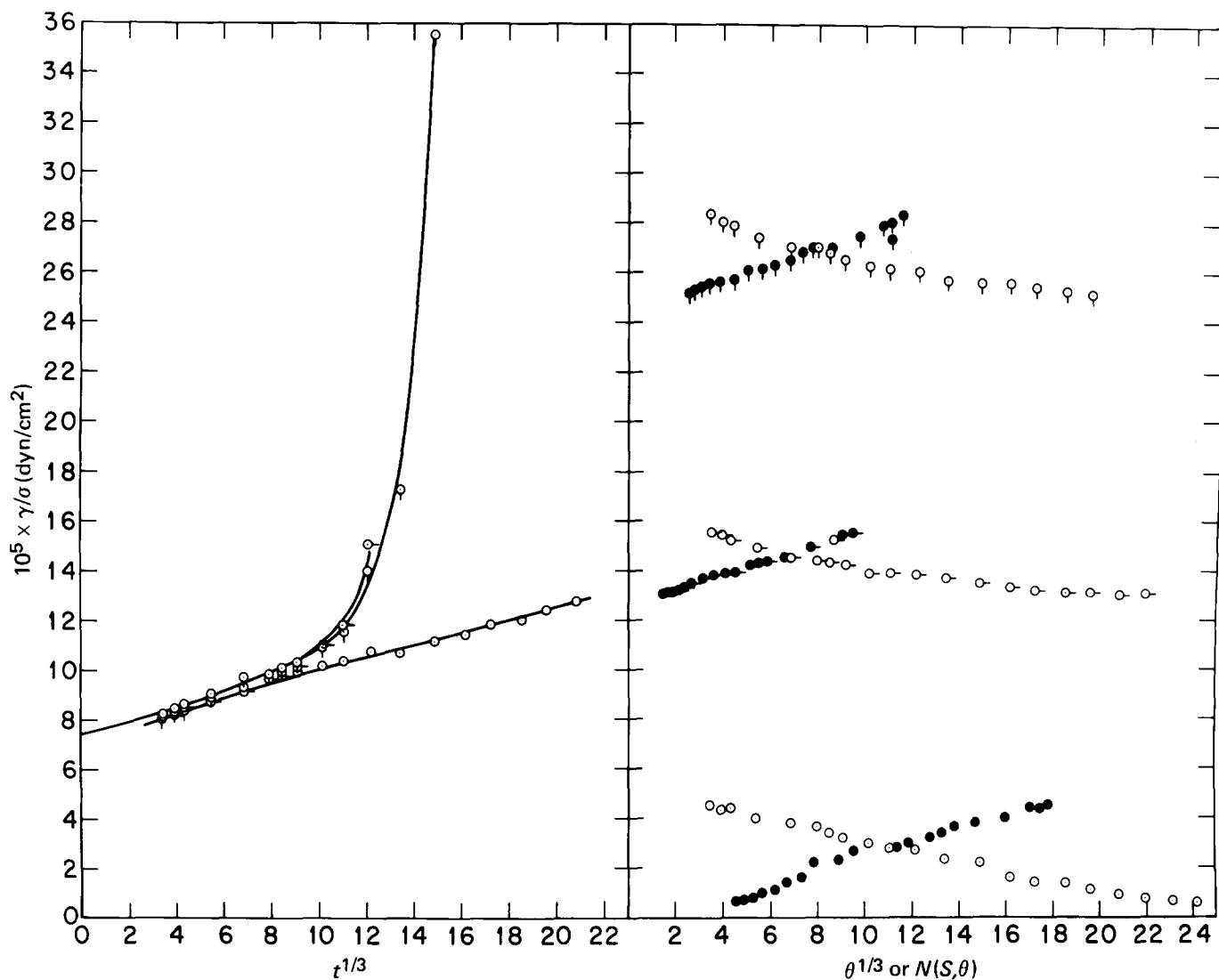


Figure 13 (a) Plot of $\gamma(t)/\sigma$ versus $t^{1/3}$ for the creep data at three stress levels: 331.7; 465.3 and 563.4 dyne/cm². (b) Plot of recoverable compliance $\gamma(\theta)/\sigma$ versus $\theta^{1/3}$ (open circles) or $N(S, \theta)$ (closed circles). Recovery from the corresponding creep shown in (a)

$J_A/\tau_A^{1/3}$ determined from creep data. Two examples of this behaviour differing in total non-recoverable strain are given in Figure 13. The solution was allowed to stand for 12 h before further testing when it was strained beyond γ_Y . Failure to allow for this aging time did not much effect J_A , but could result in erratic decrease in τ_A .

Although J_A was found to be independent of σ , and equal to 7.4×10^{-5} cm²/dyn, τ_A decreased with increasing stress. This decrease could be fitted by the relation

$$\tau_A^{-1/3} = \tau_{A0}^{-1/3} \frac{\sinh \sigma/\sigma_0}{\sigma/\sigma_0} \quad (12)$$

found to be useful in previous studies involving stress-dependent Andrade creep (see ref 6). Here, the data are fitted with equation (12) with $\tau_{A0} = 8.2 \times 10^4$ sec and $\sigma_0 = 216$ dyn/cm².

DISCUSSION

Solutions of BBB

The results with solutions of BBB in dry MSA are in accord with our previous conclusions² that such solutions ex-

hibit many of the properties found with solutions of more familiar flexible chain polymers. Thus, it was reported that the limiting viscosity at low rates of strain obeys the correlations found with many other polymers²⁰:

$$\eta_0 = (N_A/6)X(X_c)^a \zeta \quad (13)$$

with

$$\zeta = \zeta_0 \exp[C/(T - T_0)]$$

$$X = (\langle S^2 \rangle_0 / M) c Z_w$$

$$a = \begin{cases} 0 & \text{if } X \leq X_c \\ 2.4 & \text{if } X > X_c \end{cases}$$

where Z_w is the weight-average number of chain units, c is the concentration (e.g. in g/ml), and the parameters C and T_0 in the Vogel equation depend on the concentration. For many polymers, the constant X_c is about 400×10^{-17} . The principal unusual features of the behaviour observed with BBB solutions were a low value of $X_c = 12 \times 10^{-17}$ (with $\langle S^2 \rangle_0$ in cm² and $Z_w = M_w/m_a$, where the molecular weight

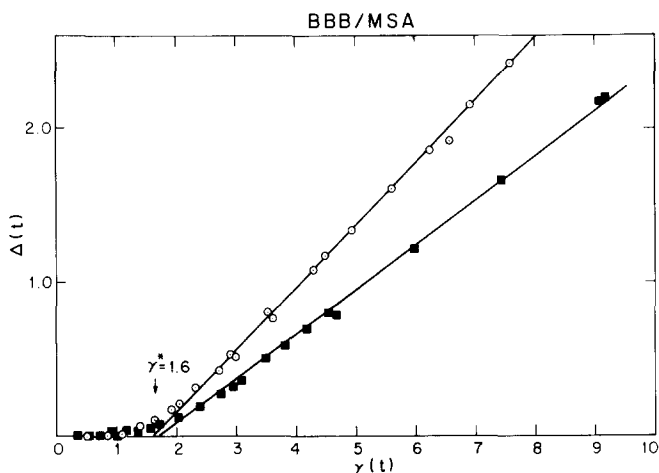


Figure 14 Deviation from linear viscoelasticity $\Delta(t)$ versus the actual strain $\gamma(t)$

m_a of a repeat unit is taken to be 410) and a marked dependence of the friction factor ζ on concentration for c greater than about 0.1 g/ml. Similarly, the present results show that the dependence of η_κ/η_0 on $\eta_0 R_0 \kappa$ is not unusual but rather that such a reduced flow curve agreed reasonably with similar data obtained⁷ with a solution of a polydisperse polyisobutylene sample.

The correlation of R_0 with molecular weight, concentration, and the molecular properties is still sufficiently crude that it is impossible to decide with certainty whether the magnitude of R_0 for the solution of BBB in dry MSA is in accord with results on other polymers. It appears that data on some systems can be correlated by an equation of the type^{13,21}

$$R_0 = R_R h(E) \quad (14)$$

with R_R the recoverable compliance calculated with the Rouse model^{13,22}:

$$R_R = 0.4(M_w/cRT)(M_{z+1} M_z/M_w^2) \quad (15)$$

and $h(E)$ a function of the entanglement density, here measured by E equal to $cM/\rho M_e$, where M_e is the molecular weight between entanglement loci. The function $h(E)$ is unity for $E \leq 1$, and a decreasing function of E for $E > 1$. The reliability of the polydispersity factor $M_z M_{z+1}/M_w^2$ in equation (15) is questionable, but used here for lack of a better estimate of the effect of molecular weight heterogeneity on R_R . Various empirical relations have been proposed^{13,21} for $h(E)$ for $E > 1$, including the simple equation

$$h(E) = kE^{-1} = \frac{k\rho M_e}{cM_w} \text{ for } E > 1 \quad (16)$$

where k is a constant. Use of equation (15) gives the result

$$c^2 R_0 = (2k\rho M_e/5RT)(M_{z+1} M_z/M_w^2) (cM_w/k\rho M_e)^b \quad (17)$$

$$b = \begin{cases} 1 & \text{if } cM_w < k\rho M_e \\ 0 & \text{if } cM_w > k\rho M_e \end{cases}$$

Thus, $c^2 R_0$ is expected to be a constant if $E > 1$. Somewhat better agreement with data is sometimes achieved with

b greater than 1 for cM_w only slightly less than $k\rho M_e$. The estimate for R_0 calculated with equation (17) for a solution of BBB in MSA ($M_w = 6.5 \times 10^4$, $c = 0.176$ g/ml and $\rho M_c = 230$) with the usual estimate $M_e = M_c/2$ and the assumption of a normal molecular weight distribution is 100-fold smaller than the observed value. This discrepancy is too large to be attributed to a molecular weight distribution broader than the assumed normal distribution, or to the failure of the factor $M_z M_{z+1}/M_w^2$ to account for the effects of molecular weight distribution on R_0 . A plausible explanation for the discrepancy is related to the unusually small value of X_c for BBB. If, as we have proposed², the latter is related to an unusually small entanglement slippage factor (Bueche's s parameter²⁰) then M_e may be much larger for BBB than the value $M_c/2$ typically observed with flexible chain polymers²⁰. Under these circumstances a better estimate for M_e for BBB might be given by $(M_c/2)(400 \times 10^{-17}/X_c)$. With this estimate of M_e in equation (20), the value calculated for R_0 (with $k = 8$) is only 2.8 times too small. The remaining discrepancy is comparable in magnitude to the uncertainty in k and the polydispersity correction applied in equation (17).

The suspected tenuous intermolecular association obtaining in solutions of BBB in dry MSA is too weak to manifest itself in yield phenomena that might be characteristic of a more tenacious aggregate structure. Rather, BBB solutions exhibit normal linear viscoelastic behaviour in the limit of small stress, described by the relation

$$\gamma(t)/\sigma = J(t) = R_0(t) + t/\eta_0 \quad (18)$$

for the creep compliance $J(t)$ where $R_0(t)$ represents the recoverable creep compliance, equal to R_0 for large t .

The systematic departure from equation (18) found at large stress and long time has precedence in solutions of other polymers^{12,14}. With those systems it was found that equation (18) was obeyed at short time at all stresses, with systematic deviations from equation (18) occurring at successively shorter times as the stress increased, just as can be seen in Figure 2 for the BBB solution in MSA. This behaviour can be revealed more clearly if the difference $\Delta(t)$ between the actual viscous strain $\gamma_\eta(t)$ and the viscous strain that would have obtained if the materials had followed equation (18) for a linear viscoelastic fluid is plotted versus the actual strain $\gamma(t)$. To compute $\Delta(t)$, we note that for a linear viscoelastic fluid $R_0(\infty, \theta) = R_0(t, \infty)$. Here we choose to use $R_0(t, \infty)$ determined from the total recoil following creep for time t in defining $\Delta(t)$ to obtain the equation

$$\Delta(t) = \gamma(t) - \sigma [R_0(t, \infty) + t/\eta_0] \quad (19)$$

Of course, at small stresses $\Delta(t)$ is zero for all σ and t . The difference $\Delta(t)$ is plotted against $\gamma(t)$ in Figure 14. It is seen that $\Delta(t)$ is zero for all σ provided $\gamma(t)$ is less than some critical value γ^* , which is about 1.6 for the BBB solution. Similar behaviour has been noted with other polymer solutions¹⁴. For $\gamma(t) > \gamma^*$, $\Delta(t)$ is an increasing function of $\gamma(t)$, eventually reaching the limiting slope of $(1 - \eta_\kappa/\eta_0)$, at steady-state, where η_κ is the viscosity at the shear rate equal to σ/η_κ . It may be noted that the points A and C in Figure 3 and the curves A and C in Figure 4 correspond to creep with $\gamma(t) < \gamma^*$, in accord with the postulate that in creep the material can be described as a linear viscoelastic fluid provided $\gamma(t) < \gamma^*$. Similarly, the points B and D in Figure 3 and the curves B and D in Figure 4 correspond to creep with $\gamma(t) > \gamma^*$ and are not in accord with the behaviour expected for a linear viscoelastic fluid.

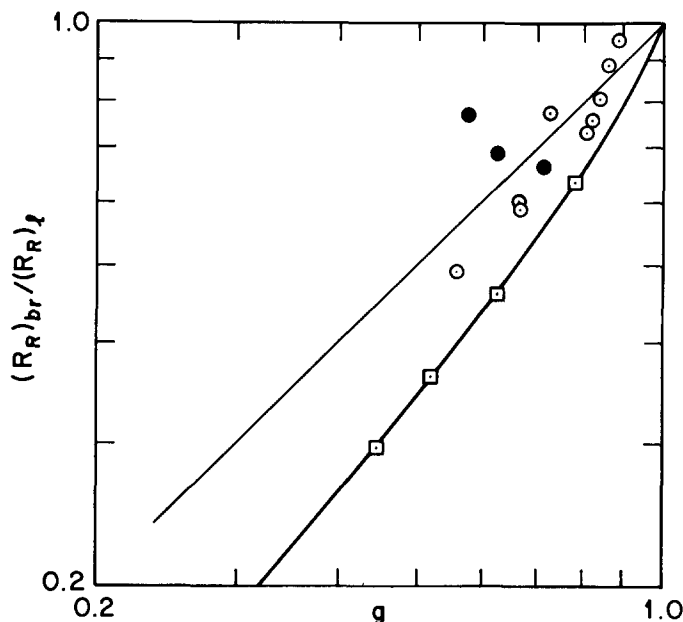


Figure 15 Plot of ratio of theoretical recoverable compliances $(R_R)_{br}/(R_R)_l$ versus g factor for various branched molecule depicted in the figure. Symbols: \square regular star; \circ irregular star and \bullet comb

The marked increase in η_0 for solutions of BBB in MSA caused by absorbed water can be understood if it is assumed that water induces random association of the polymer. Indeed, in this case the marked effect of small amounts of water affords a valuable opportunity to study the effects of such intermolecular association. This association is attributed to the deprotonation of the polymer in the presence of water. Since the polymer is weakly basic as compared with water, even small amounts of water cause appreciable deprotonation of the polymer. An approximate estimate for the magnitude of this deprotonation can be obtained through the use of the Hammett acidity function H_0 and the pK_B for the polymer. The latter was found to be about -7 for model compounds of the polymeric repeating unit², but the polymer, which is known to be more heavily protonated in sulphuric acid than the model compounds⁵, may be more basic. Thus, if C_{BH^+} and C_B are the concentrations of the protonated and deprotonated base (e.g., mol repeat unit/l), respectively, then

$$\log(C_{BH^+}/C_B) = pK_B H_0 \quad (20)$$

Data on H_0 at 25°C for methane sulphonic acid²³ and sulphuric acid²⁴ containing small amounts of water can be fitted by the empirical relation

$$H_0 = \log \left\{ 10^{H_{0,d}} + \frac{A_1 w}{1 - A_2 w} \right\} \quad (21)$$

where $H_{0,d}$ is the acidity function for the dry acid, w is the weight fraction of water and A_1 and A_2 are constants. Based on the data at 25°C, these constants are given by $H_{0,d} = -7.85$, $\log A_1 = -6.548$ and $A_2 = 10.50$ for MSA, and $H_{0,d} = -11.94$, $\log A_1 = -8.539$ and $A_2 = -12.53$ for sulphuric acid.

The fraction $m = C_B/(C_B + C_{BH^+})$ of deprotonated sites per chain, which can be approximated by C_B/C_{BH^+} in a strong acid, can be estimated with equations (20) and (21) and used to calculate the number of deprotonated sites per

molecule $v_w = mN_w$ where N_w is the weight-average chain length. The estimate will only be qualitative, however, as it does not account for the effect of temperature on H_0 , and ignores the effect of multiple protonation per repeat unit, which is known to occur with BBB in sulphuric acid⁵. With MSA, assuming that $pK_B = -6.5$, this calculation gives an increase of 2 deprotonated sites per molecule for the acid with 1.2 wt % water as compared with the dry acid, and an increase of 6 deprotonated sites per molecule for 3 wt % water content.

With the assumption that water causes random association, the increase of η_0 over the viscosity $\eta_{0,d}$ in dry MSA can be calculated with equation (13) if it is assumed that equation (13) applies for a randomly branched chain containing only a small number n_w of branches per molecule after X is generalized slightly:

$$X = (\langle S_l^2 \rangle_0 / M) c g_w Z_w (1 + n_w) \quad (22)$$

Here Z_w is the chain length of the primary chain, $\langle S_l^2 \rangle_0$ is the mean square radius of gyration of a linear chain of molecular weight, M , and g is the ratio $\langle S_l^2 \rangle_0 / \langle S_l^2 \rangle_0$ of the mean square radii of branched and linear chains at constant M . Correlation of η_0 with c , M and g in this way has precedence^{13,20} but is not always successful²⁰. Assuming random, tetrafunctional branching with²⁵

$$g_w = n_w^{-1} \ln(1 + n_w) \quad (23)$$

η_0 is given by

$$\eta_0 = \eta_{0,d} \left[\frac{1 + \eta_w}{n_w} \ln(1 + n_w) \right]^{3.4} \approx \eta_{0,d} (1 + n_w)^{1.24}$$

The approximate form of equation (24) is similar to an empirical relation introduced by Charlesby²⁶ in his studies of the viscosity of radiation grafted polymers, with the approximate form good over the interval $1 \leq (\eta_0/\eta_{0,d}) < 25$. Use of equation (24) to estimate n_w from the ratio $\eta_0/\eta_{0,d}$ for the sample with 1.2 wt % water uptake gives n_w equal to 2.5. It may be noted that n_w so calculated is about the same as the increase in v_w calculated above, as would be expected if the proposed model is reasonable. The maximum increase in η_0 shown in Figure 6 corresponds to n_w equal to 34.

The effect of the proposed association on the recoverable compliance R_0 , is less easily assessed since there is neither an adequate theory or much experimental data for use in comparisons. It might be reasonable to retain the form of equation (14), with R_R replaced by the recoverable compliance $(R_R)_{br}$ calculated with the Rouse model and with E equal to $cgM/\rho M_e$. The few available calculations of $(R_R)_{br}$ show that it is not simply related to g , but depends on other characteristics of the branched chain configuration as well. For example, the plot of $(R_R)_{br}/(R_R)_l$ versus g given in Figure 15 using values of $(R_R)_{br}$ calculated by Ham²⁷ and by Osaki and Ferry²⁸ for a few simple branched structures shows that $(R_R)_{br}/(R_R)_l$ is not a single-valued function of g . Here $(R_R)_l$ is the recoverable compliance for a linear monodisperse polymer calculated with equation (15). Inspection of Figure 15 suggests that the approximation

$$(R_R)_{br}/(R_R)_l = g_2 \approx g^\epsilon \quad (25)$$

with ϵ about equal to unity may be reasonable for comb-shaped branched molecules with a low frequency of long

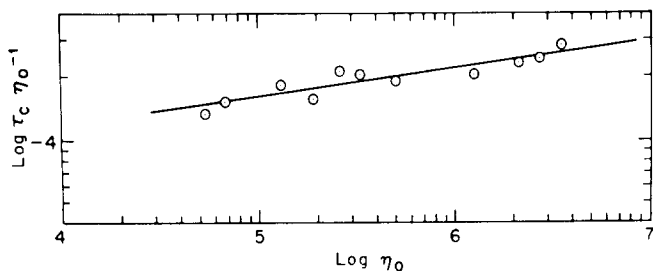


Figure 16 Logarithmic plot of R_0 as given by $\tau_c \eta_0^{-1}$ versus zero shear viscosity η_0

branches. Since such a structure might also provide a reasonable analogue to a randomly branched polymer, we will adopt equation (25), arbitrarily using the weight-average value of g . Thus for a branched polymer we find $R_0 \propto g_2/g_w = g_w^{\epsilon-1}$ if $g_w cM_w > k_p M_e$.

In using equations (24) and (25), we assume that the so-called enhancement effects reported for both η_0 and R_0 for certain branched structures^{20,31} can be ignored for the concentrated solution studied here.

Values of R_0 determined for solutions of BBB by comparison of experimental flow curves with the master curve of η_κ/η_0 versus $\eta_0 R_0 \kappa$ are plotted against η_0 in Figure 16. Viscosities are reduced to 48.9° by the a_T factors. The data are correlated by a relation of the form $R_0 \propto \eta_0^{0.14}$ or, with equations (23) and (24), $R_0 \propto g_w^{-0.27}$, in agreement with the expected dependence of R_0 on g_w if $\epsilon \sim 0.73$. Thus, the effects of small amounts of water on η_0 , R_0 and the flow curve for solutions of BBB in MSA are consistent with the postulate that the flexible chain polymer is effectively branched by loci of association created when the polymer is slightly deprotonated by the action of water.

One result that emerges from this study that bears emphasis is the relative insensitivity of the shape of the flow curve to aggregation that increased the effective molecular weight thirty-fold and the zero shear viscosity nearly one hundred-fold, e.g., the reduced curve in Figure 8. This means that with the type of aggregation studied here, one cannot determine the degree of association in a given polymer by measurement of η_κ and R_κ without additional information. On the other hand, if the aggregates dissociate on heating (or cooling) their presence may be manifested in a stronger than normal dependence of R_0 on temperature. If R_0 cannot be determined directly, the trend of the change in R_0 can be deduced from the change in $\tau_c \eta_0^{-1}$, with τ_c the shift factor required to superpose the flow curves. For example, if the aggregation follows the behaviour found here, then $R_0 \propto \eta_0^{0.14}/T \propto (1+n_w)^{0.175}/T$ for $n_w < 12$. Thus, if n_w decreased from 20 to 2 as T increased from 300 to 320K, R_0 would decrease by 40% as compared with the 6% decrease normally expected. Although this effect is much smaller than the change one would expect in η_0 , the latter is also more strongly effected by temperature *per se*, making a clear separation of the effects of temperature and dissociation difficult.

Solutions of BBL

The weight-average molecular weight of 52 000 of the BBL polymer used here corresponds to a maximum chain length of 1900 Å. In fact, some departures from a strict rod-like configuration believed to be present in BBL acts to reduce the end-to-end dimension of the sample below this value. Letting $x_w = L_w/D$, we obtain $x_w = 270$, with a molecular diameter D of 7 Å. According to Flory³⁰, a neces-

sary condition for the existence of thermodynamically stable anisotropic phase in a solution of rod-like molecules characterized by a length to diameter ratio x is that the volume fraction of polymer exceed ϕ_2^* , where

$$\phi_2^* = (8/x)(1 - 2/x) \quad (26)$$

Substitution of x_w for x in equation (26) gives a rough estimate of $\phi_2^* = 0.03$, in comparison with the actual volume fraction of 0.02 for the BBL solution used in this study. Thus, the formation of a stable anisotropic phase would not be expected according to Flory's criterion. The rheological behaviour of the BBL solution in dry MSA is in accord with this expectation. On the other hand, the rheological behaviour of solutions of BBL containing even a small amount of moisture shows conclusively that intermolecular association has taken place under the action of water. Of course, the similar molecular structure of BBB and BBL suggests that the short range character of the aggregate loci should be similar for these two polymers. However, whereas the BBB association produced a species which behaved as a randomly branched flexible chain polymer with BBL association appears to produce a 'brush-heap' aggregate structure at the polymer concentration employed here. This is distinct from the ordered phase of parallel rod-like molecules predicted by Flory under other conditions. The intramolecular inflexibility of the BBL molecule, as contrasted to the flexibility of the BBB molecule, makes the formation of the brush-heap aggregate structure possible, even at very low water content when the frequency of association per molecule is small. The intramolecular rigidity of BBL also can account for the low strain at which the aggregate structure yields, permitting non-recoverable deformation to occur.

The behaviour of the flow curves at low rates of strain for BBL solutions containing water reveals that the ruptured aggregate structure can reform on an appropriate time scale, the latter probably fixed by the rotatory diffusion constant for a BBL molecule, or more likely, for an aggregate of BBL molecules. Thus, it can be seen in Figure 9 that with the solution containing 0.5% water the viscosity is nearly inversely proportional to κ for $\kappa < 0.2 \text{ sec}^{-1}$, so that the steady-state shear stress σ_{ss} is nearly independent of κ in this range, and equal to 5 dyn/cm². For larger κ , η is independent of κ , at least over the range studied here. Non-Newtonian behaviour would be expected for large enough κ , probably with κ in the range $\kappa \sim (\eta_0 R_0)^{-1}$. Similar behaviour is observed with BBL solutions containing 1.8% water. Moreover, in this case, σ_{ss} is a little less than the measured yield stress $\sigma_Y = G_e \gamma_Y$, with σ_{ss} approaching σ_Y in the limit as κ goes to zero.

The appearance of cube-root creep at strains less than γ_Y with BBL solutions containing a small amount of water is consistent with the model usually used to understand cube-root creep and the aggregate structure proposed here. Thus, cube-root creep has been explained as the result of a stochastic process in which a few deformable sites present in the unstrained solid yield in a random fashion as the internal stress concentrates in their vicinity^{6,31}. With the ladder polymer BBL this recoverable deformation is presumed to involve the aggregate supramolecular structure, as opposed to the intramolecular effects that are important in the deformation of elastic flexible chain networks. For example, the time constant $\tau_{A0} \sim 10^5 \text{ sec}$ (1 day) for the Andrade creep is very large compared with the characteristic time τ_c of the order of 0.1 sec for viscous flow of the dry solution prior to network formation.

CONCLUSIONS

This study shows that in solution in dry MSA the heterocyclic polymer BBB follows the behaviour known for linear flexible chain polymers despite the exotic nature of the polymeric repeat unit.

The introduction of a small amount of moisture into the solution causes BBB to associate to form aggregates with the configuration of a randomly branched flexible chain polymer. The results show that a systematic study of the recoverable compliance R_0 may be the best way to assess the presence of aggregates that may be dissociated by the manipulation of some independent variable (e.g. temperature or small concentrations of an appropriate reagent).

The behaviour of BBB contrasts with that for the inflexible rod-like molecule BBL, which is structurally similar to BBB otherwise. Aggregation in BBL causes pronounced alteration in the flow curve, with the appearance of yield phenomena at relatively low degrees of association, with the yield criterion appearing to be one involving the total strain on the sample. At larger degrees of association BBL forms gels that exhibit slow Andrade creep.

ACKNOWLEDGEMENT

It is a pleasure to acknowledge the technical assistance of B. L. Hager in certain phases of this work. This study was supported in part by contract No. F33615-70-C-1058, Nonmetallic Materials Division, Air Force Materials Laboratory, Wright-Patterson Air Force Base.

REFERENCES

- 1 Van Deusen, R. L. *J. Polym. Sci. (B)* 1966, **4**, 211
- 2 Berry, G. C. *Discuss. Faraday Soc.* 1970, **49**, 121
- 3 VanDeusen, R. L., Clins, A. K. and Surei, A. J. *J. Polym. Sci. (A-1)* 1968, **6**, 1777
- 4 Wong, C. P. and Berry, G. C. *Prepr. Org. Coatings Plastics Chem. Am. Chem. Soc.*, 1973, **33**, 215
- 5 Berry, G. C. and Eisaman, P. R. *J. Polym. Sci. (Polym. Phys. Edn)* 1974, **12**, 2253
- 6 Berry, G. C. *J. Polym. Sci. (Polym. Phys. Edn)* 1976, **14**, 451
- 7 Berry, G. C. and Wong, C. P. *J. Polym. Sci. (Polym. Phys. Edn)* 1975, **13**, 1761
- 8 Leaderman, H. *J. Polym. Sci.* 1954, **13**, 371
- 9 de Witt, T. W., Markovitz, H., Padden Jr., F. J. and Zapas, L. J. *J. Colloid Sci.* 1955, **10**, 174
- 10 Prest, W. M., Porter, R. S. and O'Reilly, J. M. *J. Appl. Polym. Sci.* 1970, **14**, 2697
- 11 Markovitz, H. *J. Polym. Sci. (Polym. Symp.)* 1975, No. 50, 431
- 12 Berry, G. C., Hager, B. L. and Wong, C. -P. *Macromolecules* 1977, **10**, 361
- 13 Graessley, W. W. *Adv. Polym. Sci.* 1974, **16**, 1
- 14 Wong, C. P. and Berry, G. C. *Polym. Prepr. Am. Chem. Soc.* 1974, **15** (2), 126
- 15 Newman, A. B. *Trans. Am. Inst. Chem. Eng.* 1931, **27**, 203
- 16 Sidebottom, D. P. and Spiro, M. *J. Phys. Chem.* 1975, **79**, 943
- 17 Andrade, E. N. *Proc. Roy. Soc. (A)* 1910, **84**, 1
- 18 Ferry, J. D. 'Viscoelastic Properties of Polymers', 2nd Edn, Wiley, New York, 1970, Ch. 1
- 19 Boltzmann, L. *Akad. Wiss. Wien. Sitzber.* 1874, abt. 2, **70**, 275
- 20 Berry, G. C. and Fox, T. G. *Adv. Polym. Sci.* 1968, **5**, 261
- 21 Berry, G. C. in *Molecular Structure and the Physical Properties of Amorphous Polymeric Materials*, T. G. Fox, Spring Lecture, Am. Chem. Soc. Delaware Section (1969)
- 22 Rouse, P. E. *J. Chem. Phys.* 1953, **21**, 1272
- 23 Bascombe, K. N. and Bell, R. P. *J. Chem. Soc.* 1959, 1096
- 24 Gillespie, R. J. and Robinson, E. A. in 'Non-Aqueous Solvents' (Ed. T. C. Waddington), Academic Press, New York, 1965, Ch. 4
- 25 Zimm, B. H. and Stockmayer, W. H. *J. Chem. Phys.* 1949, **17**, 1302
- 26 Charlesby, A. and Thomas, D. *Symp. über Makromolekullen* 1959, I-C-8
- 27 Ham, J. S. *J. Chem. Phys.* 1957, **26**, 625
- 28 Osaki, K. and Schrag, J. L. *J. Polym. Sci. (Polym. Phys. Edn)* 1973, **11**, 549
- 29 Graessley, W. W. *Acc. Chem. Res.* 1977, **10**, 332
- 30 Flory, P. J. *Proc. Roy. Soc. (London)* 1956, **A234** 60, 73
- 31 Mott, N. F. *Phil. Mag.* 1953, **44**, 742